

Development of Low Dark Current SiGe Near-Infrared PIN Photodetectors on 300 mm Silicon Wafers

Caitlin Rouse¹, John W. Zeller², Harry Efstathiadis¹, Pradeep Haldar¹, Jay S. Lewis³, Nibir K. Dhar⁴, Priyalal Wijewarnasuriya⁵, Yash R. Puri², Ashok K. Sood²

¹State University of New York Polytechnic Institute, Albany, NY, USA

²Magnolia Optical Technologies Inc., Woburn, MA, USA

³DARPA/MTO, Arlington, VA, USA

⁴US Army Night Vision Sensors and Electronic Division, Fort Belvoir, VA, USA

⁵US Army Research Laboratory, Adelphi, MD, USA

Email: jwzeller@magnoliaoptical.com

Received 6 April 2016; accepted 13 May 2016; published 16 May 2016

Copyright © 2016 by authors and Scientific Research Publishing Inc.

This work is licensed under the Creative Commons Attribution International License (CC BY).

<http://creativecommons.org/licenses/by/4.0/>



Open Access

Abstract

SiGe offers a low-cost alternative to conventional infrared sensor material systems such as InGaAs, InSb, and HgCdTe for developing near-infrared (NIR) photodetector devices that do not require cooling and can operate with relatively low dark current. As a result of the significant difference in thermal expansion coefficients between germanium (Ge) and silicon (Si), tensile strain incorporated into SiGe detector devices through specialized growth processes can extend their NIR wavelength range of operation. We have utilized high throughput, large-area complementary metal-oxide semiconductor (CMOS) technology to fabricate Ge based *p-i-n* (PIN) detector devices on 300 mm Si wafers. The two-step device fabrication process, designed to effectively reduce the density of defects and dislocations arising during deposition that form recombination centers which can result in higher dark current, involves low temperature epitaxial deposition of Ge to form a thin *p*⁺ seed layer, followed by higher temperature deposition of a thicker Ge intrinsic layer. Phosphorus was then ion-implanted to create devices with *n*⁺ regions of various doping concentrations. Secondary ion mass spectroscopy (SIMS) has been utilized to determine the doping profiles and material compositions of the layers. In addition, electrical characterization of the I-V photoresponse of different devices from the same wafer with various *n*⁺ region doping concentrations has demonstrated low dark current levels (down to below 1 nA at -1 V bias) and comparatively high photocurrent at reverse biases, with optimal response for doping concentration of $5 \times 10^{19} \text{ cm}^{-3}$.

Keywords

Photodetectors, Infrared Detectors, Germanium, Photodiodes, Large-Area Wafers

1. Introduction

The increasingly widespread capability for growing germanium epitaxially on silicon in recent years has enabled the incorporation of Ge in an expanded array of detector applications. Silicon has a relatively large band gap of 1.12 eV corresponding to an absorption cutoff wavelength of ~ 1100 nm, which makes Si photodetectors unsuitable for applications requiring detection of near-infrared (NIR) wavelengths in the range of 1200 - 1600 nm and beyond. Germanium, also a group IV material, has a smaller indirect band gap of 0.66 eV. As a result, Ge absorption layers offer substantially higher optical absorption and enhanced transport properties over longer NIR wavelengths than possible with Si, making Ge based devices promising candidates for numerous applications requiring detection of NIR radiation.

Group III-V compound semiconductor and HgCdTe based infrared photodetectors offer certain advantages including high absorption efficiency, high carrier drift velocity, and mature design and fabrication technology. HgCdTe infrared photodetectors have been developed for 1 - 3, 3 - 5, and 8 - 14 μm applications, InSb for 3 - 5 μm applications, and InGaAs for ~ 1.1 - 1.7 μm applications [1]-[3]. However, III-V detectors commonly require cooling (typically down to 77 K), and integrating them into the Si complementary metal-oxide semiconductor (CMOS) process is likewise at the expense of high cost and greater complexity and can introduce doping contaminants into the devices since III-V materials can act as dopants for group IV materials [4]. Furthermore, HgCdTe detectors designed to operate at NIR wavelengths down to 1 μm normally require filtering to limit interference from longer wavelengths and consequently are relatively expensive to produce [5].

Therefore, CMOS-compatible NIR detection devices capable of operating at room temperature would offer significantly reduced size, weight, and power (SWaP) as well as lower production costs, and thus be very advantageous for a substantial number of applications. With this as our objective, we have developed uncooled detectors devices based on SiGe on leading-edge 300 mm wafers fabricated using a CMOS process. Due to their extended absorption spectrum compared to Si, Ge detector devices can provide responsivities at 1310 nm and 1550 nm that are comparable to those of commercially available InGaAs photodetectors [6]. While dark current densities reported for Ge *p-i-n* (PIN) detectors have typically exceeded those of group III-V material devices, we have developed detector devices with dark currents low enough for most pertinent sensing applications [7].

Due to their relatively high sensitivity to NIR wavelengths (particularly 1310 nm and 1550 nm), uncooled Ge based photodetectors are ideal for telecommunications related applications, as well as for enabling low-cost and high performance optical interconnections that effectively bridge Si electronics with optics [8]. Other commercial applications of interest include robot/machine vision, imaging for border surveillance and law enforcement, and biomedical applications such as spectral-domain optical coherence [9]. In addition, NIR-sensitive Ge sensors can potentially benefit military applications such as plume chemical spectra analysis and day-night vision for warfighters and ground vehicles, as well as detection of muzzle flashes and hostile mortar fire, incendiary events that emit large amounts of energy in the NIR spectral region [10].

2. Detector Design Concept

2.1. Extending NIR Operating Wavelength Range

Since the lattice constant of Ge exceeds that of Si by 4.2%, very thin epitaxial Ge layers grown on Si substrates are usually compressively strained. If a layer of epitaxial Ge is grown significantly thicker than the critical thickness of ~ 1 nm on a Si substrate at temperatures above 600°C, it will nearly completely relax [11] [12]. However, because Ge has a larger thermal expansion coefficient than Si, when the temperature is reduced to ~ 300 K after growth the consequent decrease in the lattice constant of the Ge will be suppressed by the relatively thick Si substrate. This results in generation of tensile strain in the Ge layer typically within the range of 0.15% - 0.30% [13].

Ge has a direct band gap of 0.80 eV, which is only 140 meV above its dominant indirect band gap. The presence of biaxial tensile stress in Ge causes both the direct and indirect gaps to shrink with the direct gap shrinking

faster, causing the Ge to transition from an indirect gap material towards a direct gap material [4] [13]. The incorporation of tensile strain thus offers a means of providing greater sensitivity for sensor operation at longer NIR wavelengths [14]. For example, if 0.2% tensile strain is introduced into epitaxial Ge layers, the direct band gap will reduce from 0.80 eV to ~0.77 eV, corresponding to the cutoff wavelength increasing from 1550 nm to ~1610 nm and thus providing higher optical absorption over the L band (1565 - 1625 nm) used in telecommunications [6].

2.2. Reducing Dark Current

At room temperature, leakage or dark current in PIN photodetectors is mainly generated from traps at recombination centers comprising defects and/or threading dislocations that have arisen during the growth process. Higher levels of dark current result in increased power consumption, and shot noise associated with the leakage current can also degrade the signal-to-noise ratio and lower sensitivity in NIR detectors [15]. In designing photodetectors, and in particular uncooled detectors, it is crucial to ensure that the dark current remains at an acceptable level generally considered to be 1 μ A or less [16]. Measures to potentially limit dark/leakage current include enhancing device surface and/or sidewall passivation, improving crystalline quality of material layers and adjusting the doping levels, and using optimized growth methods. It is notable that lowering band gap in Ge by incorporating tensile strain reduces the density of states for holes, leading to decreased intrinsic carrier density that can also contribute to lower reverse dark current in detector devices.

3. Device Fabrication Process

3.1. Growth/Fabrication Process Overview

We have fabricated Ge based PIN photodetector devices on 300 mm (12 inch) diameter Si wafers at the Colleges of Nanoscale Science and Engineering (CNSE), State University of New York Polytechnic Institute (SUNY Poly), located in Albany, NY. This facility offers industry-leading wafer processing technologies and high-end CMOS fabrication capabilities in fully equipped 300 mm cleanrooms with large-area Si/Ge tools, enabling epitaxial growth of Ge for the development of room temperature operation photodetectors that can be heterogeneously integrated with CMOS circuitry for significant cost reduction.

The deposition of Ge in the development of the normal-incidence PIN Ge photodetectors is accomplished through a two-step growth process intended to reduce threading dislocations arising primarily from lattice mismatch between the Si and Ge to enable higher quality Ge films with consequently lower dark current [17]. This growth technique involves initial low temperature deposition of Ge to form a thin strain-relaxed seed layer, and successive high temperature growth to form a thicker absorbing film. All Ge depositions were performed using a 300 mm reduced-pressure chemical vapor deposition (RPCVD) system utilizing germane as the precursor and hydrogen as the carrier gas with typical reactor pressures in the range of 5 - 100 Torr. The RPCVD method provides high control of layer and multi-layer thicknesses, making it well suited for large-scale wafer fabrication.

3.2. Two-Step Growth Process

The first low temperature growth step involves fully planar homoepitaxial deposition of a relatively thin Ge p^+ (boron) doped seed/buffer layer on a 300 mm Si wafer substrate at temperatures of 350°C - 400°C. At this relatively low growth temperature range intended to promote planar growth, the low surface diffusivity of Ge kinetically suppresses undesired three-dimensional Stranski-Krastanov islanding that can otherwise result from strain release [18]. By contrast, seed layer deposition at temperatures below 320°C commonly leads to crystallographic defect formation, while that at temperatures above 400°C can produce surface roughening due to the increased surface mobility of Ge [19].

In the subsequent high temperature step of the growth process, a layer of intrinsic Ge serving as the absorption region is grown at 550°C - 600°C. This temperature range was chosen to ensure satisfactory deposition rates for smooth high crystal quality Ge films with sufficient tensile strain [18]. Due to the difference in thermal expansion coefficients between the Ge and underlying Si substrate as discussed previously, compressive strain is effected in this intrinsic layer upon cooling following the high temperature growth. The wafer was later annealed at 600°C for 30 s. A flowchart illustrating the sequential device fabrication process steps is given in **Figure 1**.

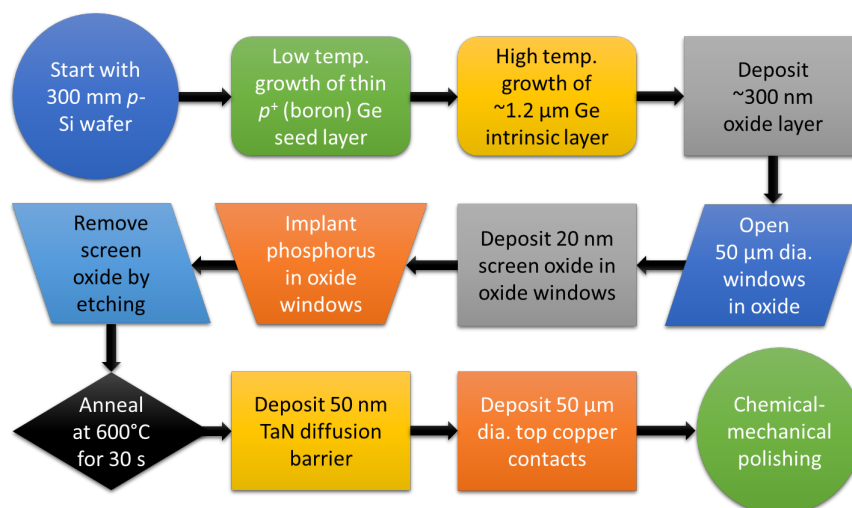


Figure 1. Flowchart illustrating device fabrication process including two-step growth.

3.3. Final Device Fabrication Steps

Following the two-step growth of the Ge seed and intrinsic layers, upper n^+ regions were formed through ion implantation of phosphorus (P) into the underlying intrinsic layer. The basic steps comprising this process are described as follows: A layer of SiO_2 was deposited above the i -Ge layer, intended to isolate states at the interface between it and the signal carrying layers as well as reduce traps that could contribute to leakage current [20]. Circular windows were then opened in this oxide to the underlying i -Ge using reactive-ion etching (RIE), in which a thin 20 nm layer of screen oxide was deposited. Next, P was ion-implanted at 60 keV through the screen oxide layer in the portions exposed by the windows, forming n^+ regions under these openings. (The processed 300 mm wafer was subjected to various degrees of P ion implantation, producing four different n^+ region doping levels in its quadrants ranging from $5 \times 10^{18} \text{ cm}^{-3}$ to $1 \times 10^{20} \text{ cm}^{-3}$.) The screen oxide was then etched away.

After formation of the n^+ regions, diffusion barrier layers composed of tantalum nitride (TaN), which is thermodynamically stable with respect to copper (Cu) and has low electrical resistance, were implemented in these openings above the n^+ regions. Finally, low resistance Cu contacts were deposited in the windows above the TaN, and chemical-mechanical polishing (CMP) was applied to the surface of the wafer/devices.

4. Device Characterization

4.1. Structural Characteristics of Devices

Various methods were utilized to characterize the material and structural properties first of the epitaxial growth and then of the fabricated detector devices. High-resolution X-ray diffraction (HRXRD) and optical microscopy demonstrated that grown epitaxial films were over-relaxed (*i.e.*, tensile strained) and composed of essentially pure Ge, having very smooth and practically defect-free topologies when the seed layers had thicknesses of at least 100 nm. By contrast, for Ge intrinsic layers grown on 22 nm thick seed layers a surface defect density of approximately 2000 cm^{-2} was observed [21].

Secondary ion mass spectroscopy (SIMS) was likewise utilized to analyze the constituent elements in the detector devices down to the Si substrate. Data representing off-contact depth analysis are plotted **Figure 2(a)**; these results show the intrinsic and seed layers of the device to be predominately comprised of Ge, and boron doping concentration of $\sim 5 \times 10^{18} \text{ cm}^{-3}$ in the latter. Through-contact SIMS data were likewise acquired, shown in **Figure 2(b)**, evidencing Ge and phosphorus underneath the contact.

4.2. Detector Electrical Performance

For testing the electrical characteristics of the fabricated photodetector devices, we utilized a probe station, electrical source-measurement unit (Keithley 2400 SourceMeter), and 10 mW broadband fiber-coupled tungsten-halogen light source providing high intensity over the NIR ($\sim 1000 - 1700 \text{ nm}$) spectrum. The dark current and

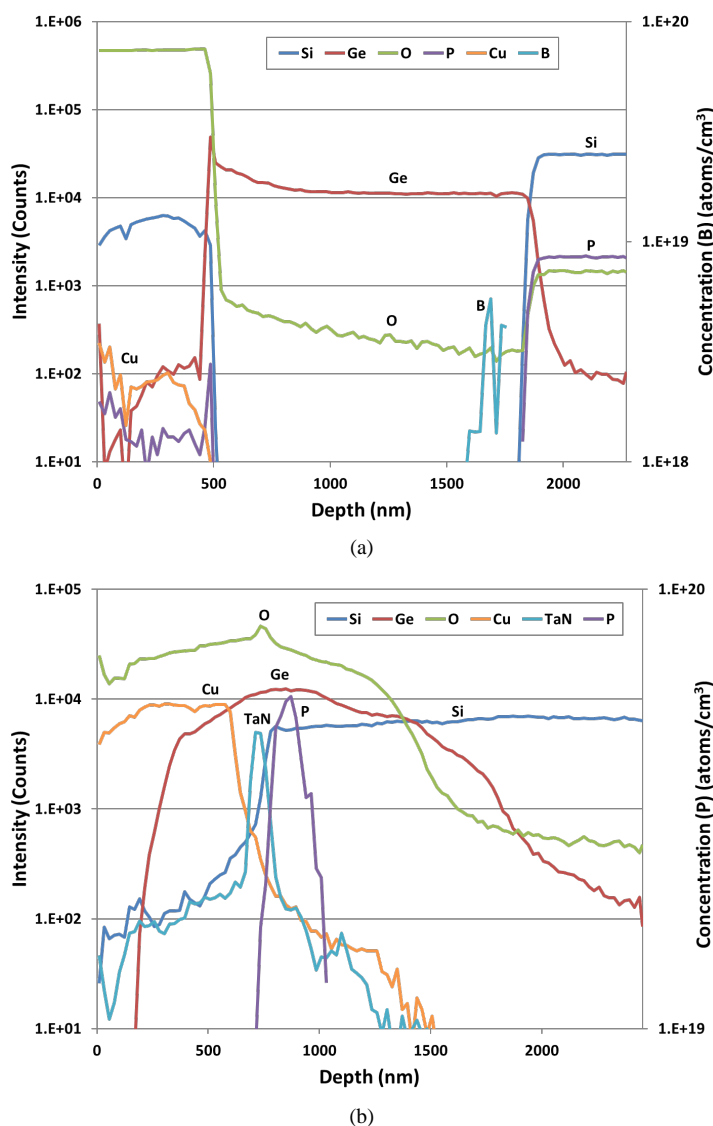


Figure 2. (a) “Off-contact” SIMS analysis data measured down through SiO_2 and the underlying PIN detector layer structure. (b) “Through-contact” SIMS analysis data measured down through Cu contact and the underlying PIN detector layer structure.

photocurrent I-V curves are shown in **Figure 3(a)**. For a device (different from the one used for SIMS data) with n^+ region P doping level of $5 \times 10^{19} \text{ cm}^{-3}$, the measured dark current at -1 V was approximately 0.6 nA , which is low compared to minimal dark current results reported to date for Ge/SiGe photodetectors [22]-[24]. For $100 \mu\text{m}$ square devices, this corresponds to a dark current density of $6 \mu\text{A}/\text{cm}^2$. Furthermore, the dark current remained relatively steady even as the magnitude of the reverse bias was increased, rising only slightly to 0.7 nA and 1.1 nA , at -2 V and -4 V , respectively.

The photocurrent at -1 V for this device was 168 nA , over two orders of magnitude greater than the dark current, which increased marginally with greater negative bias. The zero bias dark photocurrent was 138 nA , above 80% the value of that produced at -1 V . In addition, the maximum forward-to-reverse current ratio measured at $\pm 1 \text{ V}$ was $\sim 2 \times 10^5$ for a $10^{19} \text{ cm}^{-3} n^+$ -doped device.

Additionally, temporal characterization of the photoresponse for the PIN photodetector devices was performed while modulating the incident front-surface illumination on and off. **Figure 3(b)** shows the plotted photoresponse for a device with n^+ region doping of $5 \times 10^{19} \text{ cm}^{-3}$. It is seen that the dark current with no NIR

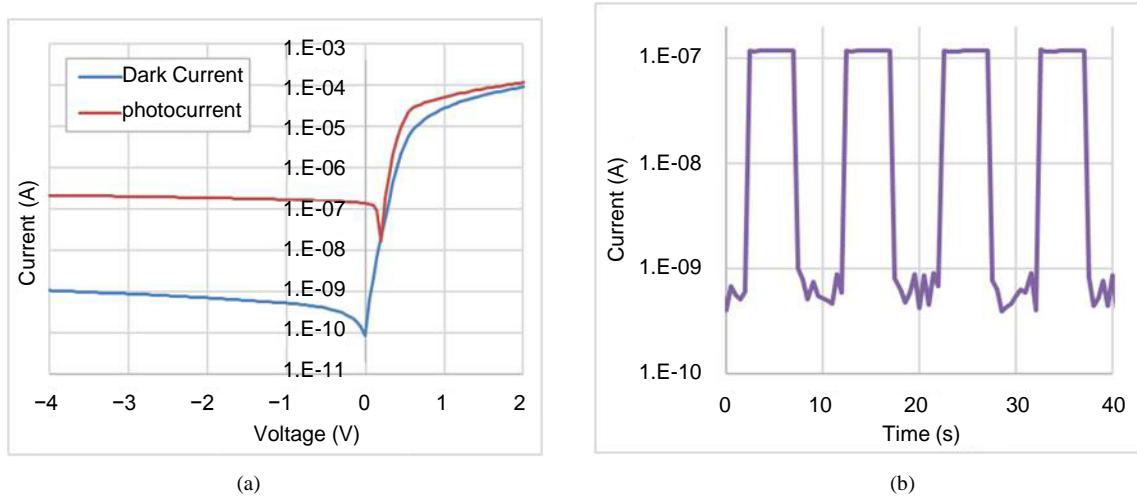


Figure 3. (a) Dark current and photocurrent I-V curves for detector device (dark current data partially extrapolated to compensate for measurement uncertainty); (b) time-dependent photoresponse measured while periodically modulating the incident NIR radiation source on and off.

Table 1. Comparison of I-V results for four devices having different n^+ region (P) doping concentrations.

Measured/Calculated Device Properties	n^+ Region Doping Levels			
	$5 \times 10^{18} \text{ cm}^{-3}$	$1 \times 10^{19} \text{ cm}^{-3}$	$5 \times 10^{19} \text{ cm}^{-3}$	$1 \times 10^{20} \text{ cm}^{-3}$
Dark Current @ -1V (nA)	1.38	1.16	0.57	1.04
Photocurrent @ -1V (nA)	56	87	168	101
Photo/Dark Ratio @ -1V	41	75	288	97
Photocurrent @0V (nA)	29	56	138	16
I_F/I_R (Dark) Ratio @ $\pm 1V$	4.6×10^4	1.9×10^5	4.8×10^4	5.1×10^3

exposure was below 1 nA. Under illumination, the measured photocurrent rose to above 100 nA, with sharp high/low transitions.

Table 1 presents a comparison of the I-V measurements and corresponding calculated values procured from fabricated photodetector devices characterized by different n^+ region doping levels. In these devices, the n -type regions must have sufficient doping (e.g., $>10^{19} \text{ cm}^{-3}$) to enable the electron transport between the metal and the semiconductor to be in the field emission regime for the creation of low-resistance ohmic contacts [25]. The ratio of photocurrent to dark current (“Photo/Dark”), for which both are measured at -1 V bias, basically constitutes the current gain of the device samples under illumination. In addition, “ I_F/I_R (Dark) Ratio” is the forward-to-reverse current ratio measured at $\pm 1 \text{ V}$ bias, where higher ratios (greater asymmetry) indicate better rectifying behavior for the PIN devices. Based on these results, the $5 \times 10^{19} \text{ cm}^{-3}$ device, which meets the above mentioned criteria for ohmic contacts, had the best overall performance including the highest photocurrent and gain, and thus is considered to have an optimal doping concentration for these types of PIN devices. The lower performance for the highest doped device may be attributed in part to less photons reaching the absorption layer due to free-carrier absorption, which increases substantially with higher doping.

5. Summary and Conclusions

Ge provides a low-cost alternative material system for developing uncooled photodetectors operating at NIR wavelengths using CMOS based fabrication processes. PIN photodetectors incorporating epitaxial Ge layers on large-area 300 mm Si substrates using leading-edge facilities and growth techniques have been developed. We have utilized a two-step low/high temperature fabrication process to reduce dark current as well as introduce tensile strain. Characterization of the material properties of fabricated detector devices evidenced high quality epitaxial growth of pure Ge. In addition, electrical characterization of devices with various n^+ region doping

concentrations demonstrated low dark currents down to ~ 0.6 nA and above two orders of magnitude enhancement in current under broadband illumination at -1 V bias, with $5 \times 10^{19} \text{ cm}^{-3}$ identified to be the optimal n^+ doping level. Arrays developed based on such NIR photodetectors exhibiting low dark current could potentially benefit applications such as muzzle flash or hostile fire detection for which low noise background is desired.

6. Future Work

Each fabricated wafer contains hundreds of different devices which we characterize via SIMS and electrical measurements. Due to the difficulty of maintaining control over Ge etching, further investigation mainly employing transmission electron microscopy (TEM) is needed in order to confirm the uniformity of the Ge in different devices across the wafer.

Acknowledgements

This research was developed with funding from the Defense Advanced Research Projects Agency (DARPA). The views, opinions, and/or findings expressed are those of the authors and should not be interpreted as representing the official views or policies of the Department of Defense or the US Government.

References

- [1] Stobie, J., Hairston, A., Tobin, S., Reine, M., Minich, B., Welsch, J. and Marciniak, J. (2007) VLIWR HgCdTe Staring Focal Plane Array Development. *Proceedings of SPIE*, San Diego, 26 August 2007, 66600L-66600L.
- [2] Rawe, R., Timlin, A., Davis, M., Devitt, J. and Greiner, M. (2004) Advanced Large-Format InSb FPA Maturation at CMC Electronics. *Proceedings of SPIE*, Orlando, 30 August 2004, 152-162.
- [3] Onat, B.M., Huang, W., Masaun, N., Lange, M., Ettenberg, M.H. and Dries, C. (2007) Ultra-Low Dark Current In-GaAs Technology for Focal Plane Arrays for Low-Light Level Visible-Shortwave Infrared Imaging. *Proceedings of SPIE*, Orlando, 9 April 2007, 152-162. <http://dx.doi.org/10.1117/12.720522>
- [4] Wang, J. and Lee, S. (2011) Ge-Photodetectors for Si-Based Optoelectronic Integration. *Sensors*, **11**, 696-718. <http://dx.doi.org/10.3390/s110100696>
- [5] Hansen, M.P. and Malchow, D.S. (2008) Overview of SWIR Detectors, Cameras, and Applications. *Proceedings of SPIE*, Orlando, 16 March 2008, 69390I-69390I.
- [6] Liu, J., Cannon, D.D., Wada, K., Ishikawa, Y., Jongthammanurak, S., Danielson, T., Michel, J. and Kimerling, L.C. (2005) Tensile Strained Ge p-i-n Photodetectors on Si Platform for C and L Band Telecommunications. *Applied Physics Letters*, **87**, 011110. <http://dx.doi.org/10.1063/1.1993749>
- [7] Morse, M., Dosunmu, O., Sarid, G. and Chetrit, Y. (2006) Performance of Ge-on-Si p-i-n Photodetectors for Standard Receiver Modules. *IEEE Photonics Technology Letters*, **8**, 2442-2444. <http://dx.doi.org/10.1109/LPT.2006.885623>
- [8] Okyay, A.K. (2007) Si-Ge Photodetection Technologies for Integrated Optoelectronics. Ph.D. Thesis, Stanford University.
- [9] Rogalski, A. (2012) Progress in Focal Plane Array Technologies. *Progress in Quantum Electronics*, **36**, 342-473. <http://dx.doi.org/10.1016/j.pquantelec.2012.07.001>
- [10] Sood, A.K., Richwine, R.A., Sood, A.W., Puri, Y.R., DiLello, N., Hoyt, J.L., Akinwande, T.I., Dhar, N.K., Balcerak, R.S. and Bramhall, T.G. (2011) Characterization of SiGe-Detector Arrays for Visible-NIR Imaging Sensor Applications. *Proceedings of SPIE*, Orlando, 25 April 2011, 801240-801240. <http://dx.doi.org/10.1117/12.889205>
- [11] Feng, D., Shirong, L., Dong, P., Feng, N.N., Liang, H., Zheng, D., Kung, C.C., Fong, J., Shafiiha, R., Cunningham, J., Krishnamoorthy, A.V. and Asghari, M. (2009) High-Speed Ge Photodetector Monolithically Integrated with Large Cross-Section Silicon-on-Insulator Waveguide. *Applied Physics Letters*, **95**, 261105. <http://dx.doi.org/10.1063/1.3279129>
- [12] Luong, K.P., Dau, M.T., Zrir, M.A., Stoffel, M., Le Thanh, V., Petit, M., Ghrib, A., El Kurdi, M., Boucaud, P., Rinnert, H. and Murota, J. (2013) Control of Tensile Strain and Interdiffusion in Ge/Si(001) Epilayers Grown by Molecular-Beam Epitaxy. *Journal of Applied Physics*, **114**, 083504. <http://dx.doi.org/10.1063/1.4818945>
- [13] Liu, J., Camacho-Aguilera, R., Bessette, J.T., Sun, X., Wang, X., Cai, Y., Kimerling, L.C. and Michel, J.F. (2012) Ge-on-Si Optoelectronics. *Thin Solid Films*, **520**, 3354-3360. <http://dx.doi.org/10.1016/j.tsf.2011.10.121>
- [14] Ishikawa, Y. and Wada, K. (2010) Germanium for Silicon Photonics. *Thin Solid Films*, **518**, S83-S87. <http://dx.doi.org/10.1016/j.tsf.2009.10.062>
- [15] DiLello, N.A. (2012) Fabrication and Characterization of Germanium-on-Silicon Photodiodes. Ph.D. Thesis, Massa-

chusetts Institute of Technology.

- [16] Ahn, D., Hong, C., Liu, J., Giziewicz, W., Beals, M., Kimerling, L., Michel, J., Chen, J. and Kartner, F.X. (2007) High Performance, Waveguide Integrated Ge Photodetectors. *Optics Express*, **15**, 3916-3921. <http://dx.doi.org/10.1364/OE.15.003916>
- [17] Luan, H.C., Lim, D.R., Lee, K.K., Chen, K.M., Sandland, J.G., Wada, K. and Kimerling, L.C. (1999) High-Quality Ge Epilayers on Si with Low Threading-Dislocation Densities. *Applied Physics Letters*, **75**, 2909-2911. <http://dx.doi.org/10.1063/1.125187>
- [18] Michel, J., Liu, J. and Kimerling, J.C. (2010) High-Performance Ge-on-Si Photodetectors. *Nature Photonics*, **4**, 527-534. <http://dx.doi.org/10.1038/nphoton.2010.157>
- [19] Olubuyide, O., Danielson, D., Kimerling, L. and Hoyt, J. (2006) Impact of Seed Layer on Material Quality of Epitaxial Germanium on Silicon Deposited by Low Pressure Chemical Vapor Deposition. *Thin Solid Films*, **508**, 14-19. <http://dx.doi.org/10.1016/j.tsf.2005.06.120>
- [20] Sood, A.K., Zeller, J.W., Richwine, R.A., Puri, Y.R., Efstathiadis, H., Haldar, P., Dhar, N.K. and Polla, D.L. (2015) Ge Based Visible-NIR Photodetector Technology for Optoelectronic Applications. In: Yasin, M., Arof, H. and Harun, S.W., Eds., *Advances in Optical Fiber Technology: Fundamental Optical Phenomena and Applications*, Intech, Rijeka, 315-361.
- [21] Zeller, J.W., Efstathiadis, H., Bhowmik, G., Haldar, P., Dhar, N.K., Lewis, J., Wijewarnasuriya, P., Puri, Y.R. and Sood, A.K. (2015) Development of Ge PIN Photodetectors on 300 mm Si Wafers for Near-Infrared Sensing. *International Journal of Engineering Research and Technology*, **8**, 23-33.
- [22] Beals, M., Michel, J., Liu, J.F., Ahn, D.H., Sparacin, D., Sun, R., Hong, C.Y., Kimerling, L.C., Pomerene, A., Carothers, D., Beattie, J., Kopa, A., Apsel, A., Rasras, M.S., Gill, D.M., Patel, S.S., Tu, K.Y., Chen, Y.K. and White, A.E. (2008) Process Flow Innovations for Photonic Device Integration in CMOS. *Proceedings of SPIE*, San Jose, 19 January 2008, 689804-689804. <http://dx.doi.org/10.1117/12.774576>
- [23] Chen, H.T., Verheyen, P., De Heyn, P., Lepage, G., De Coster, J., Absil, P., Roelkens, G. and Van Campenhout, J. (2015) High-Responsivity Low-Voltage 28-Gb/s Ge p-i-n Photodetector with Silicon Contacts. *Journal of Lightwave Technology*, **33**, 820-824. <http://dx.doi.org/10.1109/JLT.2014.2367134>
- [24] Koester, S.J., Schow, C.L., Schares, L., Dehlinger, G., Schaub, J.D., Doany, F.E. and John, R.A. (2007) Ge-on-SOI-Detector/Si-CMOS-Amplifier Receivers for High-Performance Optical-Communication Applications. *Journal of Lightwave Technology*, **25**, 46-57. <http://dx.doi.org/10.1109/JLT.2006.888923>
- [25] Dumas, C.S. (2015) Germanium on Silicon Photonics. Ph.D. Thesis, University of Glasgow, Scotland.